physchem

MDPI

Article

Enhanced Circularly Polarized Luminescence and Thermal Stability of Eu(*D*-facam)$_3$ in Imidazolium-Based Ionic Liquid EMImOAc

Arata Suzuki, Ziying Li, Norihisa Kobayashi and Kazuki Nakamura *

Graduate School of Engineering, Chiba University, 1-33 Yayoi-cho, Inage-ku, Chiba-shi 263-8522, Chiba, Japan
* Correspondence: nakamura.kazuki@faculty.chiba-u.jp

Abstract

The optical and thermal behaviors of a chiral europium(III) β-diketonate complex, Eu(*D*-facam)$_3$ (facam: 3-(trifluoromethylhydroxymethylene)-(+)-camphorate), were examined in the presence of imidazolium-based ionic liquid 1-ethyl-3-methylimidazolium acetate (EMImOAc). The addition of EMImOAc to Eu(*D*-facam)$_3$ butanol solutions enhanced their luminescence intensity by up to 74-fold and induced clear circularly polarized luminescence ($g_{CPL} = -0.28$ for the $^5D_0 \rightarrow {}^7F_1$ transition). When Eu(*D*-facam)$_3$ was dissolved directly in EMImOAc, the Eu(III) complex also exhibited distinct circularly polarized luminescence ($g_{CPL} = -0.22$). In addition, compared with the thermal stability of luminescence in 1-butanol, the ionic liquid solution exhibited superior thermal robustness, retaining approximately 30% of its room-temperature emission intensity even at 100 °C. Arrhenius analysis of the solutions was performed using their emission intensity and lifetime to evaluate the emission stability at higher-temperature regions near 70–100 °C. In EMImOAc, the thermal acceleration of the nonradiative decay of the ligands was suppressed; thus, the energy transfer from the ligand to the Eu(III) ion was stabilized even at higher temperatures. These results highlight the role of ionic liquids as effective media toward achieving thermally robust and highly emissive chiral Eu(III) systems.

Keywords: europium(III) complex; circularly polarized luminescence; ionic liquid; luminescent material; thermal stability

Check for updates

Academic Editors: Paulo Ernesto Marchezi and Eralci Moreira Therézio

Received: 20 December 2025
Revised: 28 January 2026
Accepted: 13 February 2026
Published: 25 February 2026

Copyright: © 2026 by the authors. Licensee MDPI, Basel, Switzerland. This article is an open access article distributed under the terms and conditions of the Creative Commons Attribution (CC BY) license.

1. Introduction

Lanthanide ions have attracted considerable attention as photofunctional materials for a wide range of applications, including organic light-emitting diodes (OLEDs) [1,2] and bioanalytical and medical technologies [3–5]. This is primarily due to their unique 4f electronic configuration, which is effectively shielded from the external environment and consequently leads to exceptional optical properties such as high color purity and long luminescence lifetimes.

In recent years, significant progress has been made in the use of lanthanide complexes for the recognition of chiral environments based on their luminescent properties, and their applications have expanded to areas such as bioanalysis and advanced sensing technologies [6]. In studies on chiral recognition, the differential molecular response to circularly polarized light is particularly important. Among them, circular dichroism (CD) and circularly polarized luminescence (CPL) are complementarily used as probes reflecting the chiral structures of the ground and excited states, respectively.

Although CD spectroscopy is widely employed, its signals can become extremely weak when the target molecules exhibit insufficient absorption. Therefore, enhancing the CD response by introducing chromophoric units is an effective strategy [7]. Owing to their high luminescence efficiency and flexible coordination behavior, lanthanide complexes are highly promising building blocks for constructing chiroptical-responsive systems [3].

CPL has also attracted considerable attention as a sensitive probe for local chiral environments, and the degree of emission asymmetry can be quantitatively described by

$$g_{\mathrm{CPL}} = \frac{2(I_L - I_R)}{I_L + I_R} \quad (1)$$

where I_L and I_R are the intensities of left- and right-handed circularly polarized emissions, respectively. In particular, numerous chiral lanthanide complexes have been reported to exhibit g_{CPL} values exceeding 0.1, which are more than an order of magnitude higher than those typically observed for organic molecules [8–10]. Interest in chiral lanthanide complexes as promising CPL emitters has been further motivated by the development of high-resolution three-dimensional display technologies [11].

β-Diketonate lanthanide complexes that exhibit a combination of chirality and luminescent functionality represent highly attractive material platforms. Among them, Eu(*D*-facam)$_3$, which incorporates a chiral camphor-derived ligand (facam: 3-(trifluoromethylhydroxymethylene)-(+)-camphorate) and exhibits CPL activity, is one of the most representative complexes. However, its relatively low emission efficiency and insufficient thermal stability are major challenges to its practical application [12].

To further exploit the luminescent properties of Eu(*D*-facam)$_3$, numerous studies have focused on achieving strong emission, pronounced CPL, and enhanced thermal stability in various composite systems [12–14]. One important strategy is the realization of high luminescence performance in ionic environments, which is essential for the application of lanthanide complexes in electrochemical devices and bio-related fields. However, Raman spectroscopy and DFT (Density Functional Theory) calculations have demonstrated that, in high-ionic strength media, electrostatic interactions with surrounding ions affect the coordination sphere of Ln^{3+} ions. This interaction weakens the ligand coordination and may promote complex dissociation [15].

However, recent studies have reported that the appropriate control of the complex structure and its surrounding environment can lead to improved luminescence, even under such ionic conditions. In our previous work, we demonstrated that the incorporation of ionic alkylammonium salts into Eu(*D*-facam)$_3$ significantly enhanced both emission intensity and CPL activity [12,16,17].

In this study, we investigated the incorporation of Eu(*D*-facam)$_3$ into an ionic liquid (IL), which possesses outstanding physicochemical properties. ILs exhibit a wide liquid-phase temperature range, high thermal stability, nonvolatility, and excellent solvation abilities for various solutes [18,19]; therefore, they are expected to exert beneficial effects on the stability and optical responsiveness of lanthanide complexes. Indeed, Eu(III) complexes stabilized in ILs have been reported to exhibit reversible electrochemically controlled luminescence switching based on the intrinsic Eu^{3+}/Eu^{2+} redox process [20]. It has been reported that hybridization of the Eu(*D*-facam)$_3$ with alkylammonium acetate significantly enhances the luminescent properties of Eu(*D*-facam)$_3$ [12,16,17]. The IL used in this study, 1-ethyl-3-methylimidazolium acetate (EMImOAc), contains the same acetate anion (OAc^-) and is likewise expected to influence the optical properties of the Eu complex through electrostatic and/or coordinative interactions.

Accordingly, the present work aims to investigate in detail the structural and photophysical properties of Eu(*D*-facam)$_3$ in the presence of EMImOAc, with a particular focus on the enhancement of luminescence intensity, CPL activity, and thermal stability.

Figure 1 shows the molecular structures of the chiral Eu(*D*-facam)$_3$ complex and the ionic liquid, EMImOAc, investigated in this study.

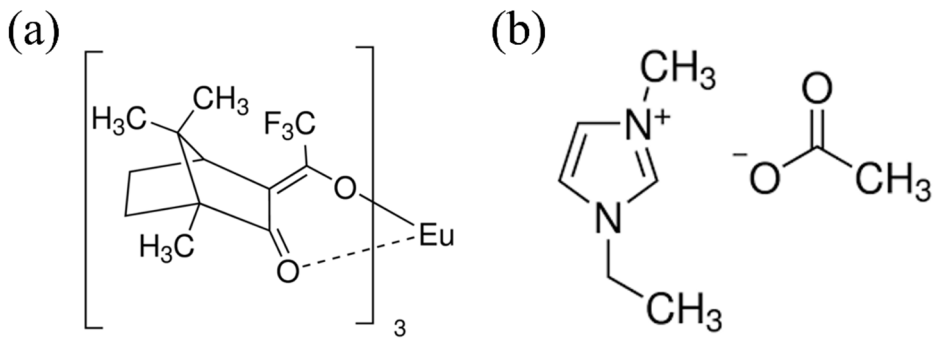

Figure 1. Chemical structure of (**a**) Eu(*D*-facam)$_3$ and (**b**) EMImOAc.

2. Experimental Section

2.1. Reagents

All chemicals were commercially available and used as received. Eu(*D*-facam)$_3$ was purchased from Sigma-Aldrich, Tokyo, Japan. EMImOAc and 1-butanol were purchased from Tokyo Chemical Industry Co., Ltd. (TCI, Tokyo, Japan).

2.2. Preparation of Eu(D-facam)$_3$ Solutions

A 1-butanol solution was prepared as the standard reference by dissolving Eu(*D*-facam)$_3$ (0.2 mM) in 1-butanol. This solution was referred to as Sol. A (Eu in BuOH). When Eu(*D*-facam)$_3$ and EMImOAc were co-dissolved in 1-butanol, the concentration of Eu(*D*-facam)$_3$ was fixed at 0.2 mM, while the concentration of EMImOAc was systematically varied. This series of solutions is denoted as Sol. B (*x*:*y*), where *x*:*y* represents the molar ratio of [Eu(*D*-facam)$_3$]:[EMImOAc] (e.g., Sol. B (1:50)). The IL solution prepared by dissolving Eu(*D*-facam)$_3$ directly into EMImOAc at a molar ratio of 1:200 is referred to as Sol. C (Eu in IL).

2.3. Photophysical Measurements

Any dissolved oxygen present in the Eu(*D*-facam)$_3$/EMImOAc solutions was removed by bubbling nitrogen gas through the solution prior to the optical measurements. The absorption and CD spectra of the Eu(*D*-facam)$_3$/EMImOAc solutions were recorded using a CD spectrophotometer (J-1100, JASCO Corporation, Tokyo, Japan). The photoluminescence (PL) spectra were obtained using a spectrofluorometer (FP-6800, JASCO Corporation, Tokyo, Japan). The emission lifetimes were measured using a fluorescence lifetime spectrometer (Quantaurus-Tau C11367-21, Hamamatsu Photonics K.K., Hamamatsu, Japan), and the emission quantum yields were calculated from the data obtained using an absolute PL quantum yield spectrometer (Quantaurus-QY C11347-01, Hamamatsu Photonics K.K., Hamamatsu, Japan). CPL measurements were performed using a previously reported system [21]. This system consisted of a 375 nm LED light source (M365L2, Thorlabs Japan Inc., Tokyo, Japan), an LED driver (DC2100, Thorlabs Japan Inc., Tokyo, Japan), a photoelastic modulator (PEM-90, Hinds Instruments Inc., Hillsboro, OR, USA), a photomultiplier tube (H7732-10, Hamamatsu Photonics K.K., Hamamatsu, Japan), a linearly polarized cube prism (200,000:1), and a dual-phase DSP lock-in amplifier (7265, Signal Recovery Ltd., Oak Ridge, TN, USA). The detection wavelengths of the monochromator and the PEM were controlled using a PC (Dell D11M). The temperature of the temperature-dependent

emission measurements was controlled using a CoolSpeK UV/CD system (USP-203 Series, Unisoku Co., Ltd., Osaka, Japan). Prior to the temperature-dependent measurements, all samples were subjected to an annealing treatment at 100 °C for 90 min.

3. Result and Discussion

3.1. Effect of IL Mixing Ratio on the Photophysical Behavior of Eu(D-facam)$_3$ in 1-butanol

Upon the addition of EMImOAc to the Eu(*D*-facam)$_3$ butanol solution, a slight increase in ligand absorbance at approximately 310 nm was observed in the absorption spectra, while the CD spectra also changed, including a decrease and increase in the Cotton effect in the shorter- and longer-wavelength regions, respectively (Figure S1). These results suggest that the local coordination symmetry around the Eu^{3+} ion and the chirality of the complex are affected by the interactions between the Eu complex and IL.

Figure 2a shows the emission spectra of Eu(*D*-facam)$_3$ in 1-butanol upon excitation at 350 nm. The emission intensity was markedly enhanced with the addition of EMImOAc, exhibiting up to a 74-fold increase (Figure 2b). To examine whether the observed enhancement in emission intensity originates from changes in light absorption, the optical densities at the excitation wavelength (350 nm) were evaluated for representative samples. The optical density at 350 nm was 0.062 for Sol. A (Eu in BuOH) and 0.075 for Sol. B (1:50), indicating only a minor difference in absorption upon the addition of EMImOAc. All emission measurements were performed under strictly identical instrumental conditions, including the excitation light intensity, detector sensitivity, optical slit widths, and integration time, without any normalization of the excitation intensity. Therefore, the pronounced enhancement in emission intensity cannot be attributed to increased absorption of the excitation light or changes in measurement conditions. Figure 2c shows the relative intensity (I_{rel}) of the electric-dipole transition at approximately 613 nm normalized to the magnetic-dipole transition at approximately 590 nm for each mixing ratio. I_{rel} is widely used as an indicator of the local coordination environment of lanthanide ions, since the magnetic-dipole transition is essentially insensitive to the coordination environment, whereas the electric-dipole transition is highly sensitive to the local coordination symmetry around the Eu^{3+} ion. I_{rel} increased sharply upon the addition of five equivalents of EMImOAc and continued to gradually increase at higher concentrations. These results indicate a reduction in the local coordination symmetry around the Eu^{3+} ion, which increases the electric-dipole contribution to the f–f transitions, thereby enhancing the transition probability of these parity-forbidden transitions under higher symmetry. An increase in the transition probability enhances the luminescence intensity of the Eu(III) complex. These structural changes induced by the addition of the IL are consistent with the findings by Puntus et al. [22]. They demonstrated that the luminescence behavior of Eu(III) complexes in ILs is strongly influenced by the strength of the cation–anion interactions, as well as by the molecular size and coordinating ability of the anion. EMImOAc contains a small and strongly coordinating carboxylate anion, which can alter the local coordination environment around Eu^{3+} and suppress vibrational quenching caused by –OH groups in 1-butanol. These effects are likely responsible for the observed enhancement in emission intensity.

To obtain complementary evidence for structural association between Eu(*D*-facam)$_3$ and EMImOAc, we also examined the system by ESI-MS (Figure S3). Spectroscopic identification of subtle coordination changes by IR spectroscopy was considered; however, acetate-related vibrational shifts associated with weak or partial interactions are difficult to resolve in solution, and vibrational modes involving Eu–O coordination are expected to appear in the low-frequency region (around 500 cm^{-1}), which is beyond the accessible range of our IR setup.

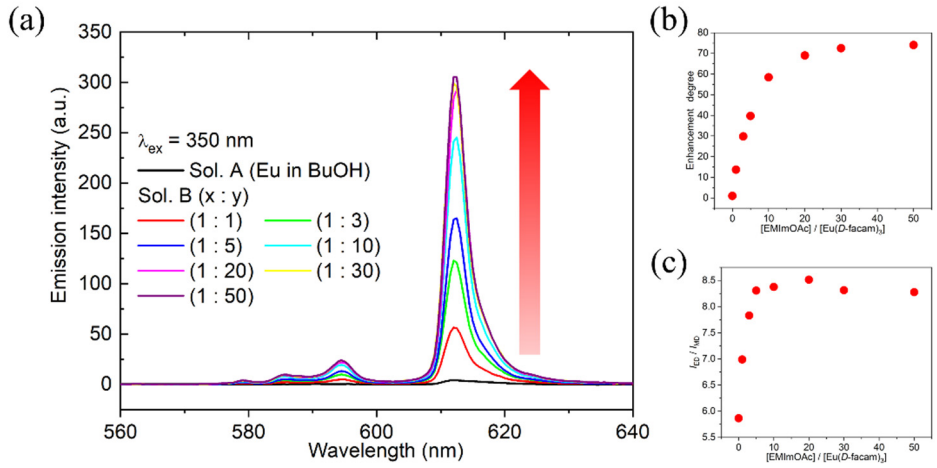

Figure 2. (**a**) Emission spectra of Sol. A (Eu in BuOH) and Sol. B with varying EMImOAc concentrations (λ_{ex} = 350 nm). (**b**) Enhancement degree of the 612 nm electric-dipole emission as a function of EMImOAc equivalents. (**c**) Relative intensity ratio of the electric-dipole to magnetic-dipole emissions ($I_{rel} = I_{ED}/I_{MD}$) as a function of EMImOAc equivalents.

As an alternative and complementary approach, ESI-MS was therefore employed. In the negative-ion mode of Sol. A (Eu in BuOH), the spectrum is dominated by signals attributable to the *D*-facam ligand and related fragment ions. In contrast, Sol. B (1:50) exhibits an additional peak assignable to a Eu(*D*-facam)$_3$·OAc$^-$ species, indicating association between the Eu(III) complex and acetate anions.

Furthermore, in the positive-ion mode of Sol. B (1:50), signals corresponding to Eu(*D*-facam)$_3$·2EMIm$^+$·OAc$^-$ adduct species were observed, whereas such features were absent in Sol. A. These results suggest that Eu(*D*-facam)$_3$ is capable of forming associated species with acetate anions and EMIm$^+$ cations in solution.

Although these measurements were performed in an alcohol-based medium and do not directly establish the coordination structure in neat EMImOAc, the observed adduct ions support the presence of specific interactions between Eu(*D*-facam)$_3$ and EMImOAc components, consistent with the proposed perturbation of the local coordination environment around the Eu^{3+} ion.

Figure 3 shows the emission decay profiles of Eu(*D*-facam)$_3$ in 1-butanol for the $^5D_0 \rightarrow {}^7F_2$ transition (612 nm). Upon the addition of EMImOAc, the decay behavior changed markedly, with the short-lived component being suppressed, allowing the decay curves to be well fitted by a single-exponential function with a longer lifetime. This behavior suggests that the luminescent environment of the Eu(III) complexes in solution became more homogeneous [23,24]. Furthermore, the average emission lifetime was significantly prolonged by the addition of EMImOAc. Specifically, the average emission lifetime of the Eu(*D*-facam)$_3$ solution increased from 66.0 μs in the absence of the IL to 112 μs when 50 equivalents of EMImOAc were added. This indicates a suppression of nonradiative deactivation processes from the $^5D_0$ excited state of the Eu(III) ion. It is likely that electrostatic interactions between EMImOAc and Eu(*D*-facam)$_3$ lead to the formation of a protective environment around the complex, thereby suppressing vibrational quenching induced by the –OH groups of 1-butanol [25,26].

Figure 4 shows the CPL spectra of Eu(*D*-facam)$_3$ in 1-butanol with varying EMImOAc concentrations. Although no CPL signal was observed for Eu(*D*-facam)$_3$ alone, the addition of EMImOAc induced a clear CPL response. This emergence of CPL is consistent with the changes observed in the CD spectra and suggests that the introduction of EMImOAc alters the coordination environment and chirality of the Eu(III) complex. The sensitivity of the CPL to subtle electronic and geometric perturbations within the coordination sphere

has been demonstrated in related Eu(III) systems. Hasegawa et al. [10] reported that even slight variations in ligand or counter-ion interactions can modify the electric and magnetic transition dipole moments through LMCT mixing, resulting in enhanced g_{CPL} values of up to −1.54. This mechanism is directly relevant to the present system, as the involvement of EMImOAc is expected to induce analogous perturbations around the Eu^{3+} center. In line with this mechanism, the luminescence dissymmetry factor (g_{CPL}), an intensity-independent parameter for CPL, reached −0.28 for the $^5D_0 \rightarrow {}^7F_1$ transition, indicating pronounced chiroptical emission properties. As discussed above, the changes in I_{rel} and CD spectra indicate a reorganization of the local coordination environment around the Eu^{3+} ion induced by interactions with EMImOAc. In our previous study, we found that the interaction between alkylammonium acetate and Eu(*D*-facam)$_3$ in 1-butanol solutions leads to an enhancement of the luminescence properties [17]. In the present system, similar interactions and associated changes in the local coordination environment are considered to occur. The activation of CPL is likely caused by such local structural reorganization, which modulates the chiral coordination environment of the complex.

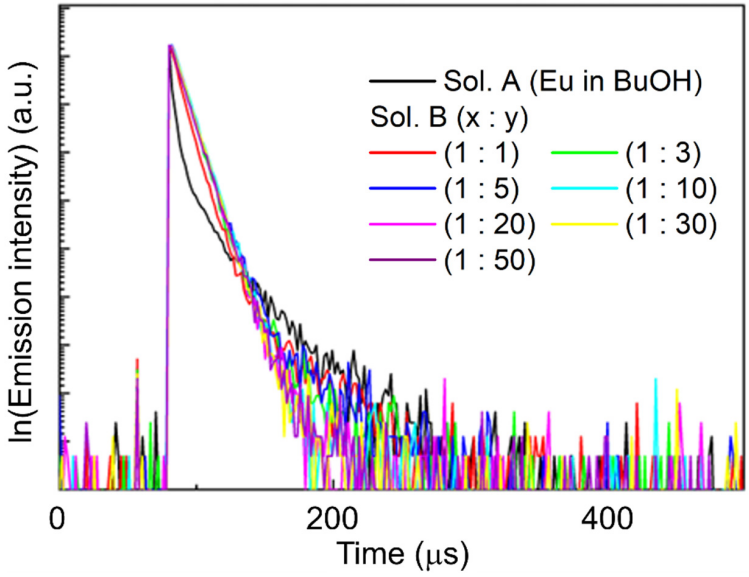

Figure 3. Emission decay profiles of Sol. A (Eu in BuOH) and Sol. B with varying EMImOAc concentrations (λ_{ex} = 340 nm; λ_{em} = 612 nm).

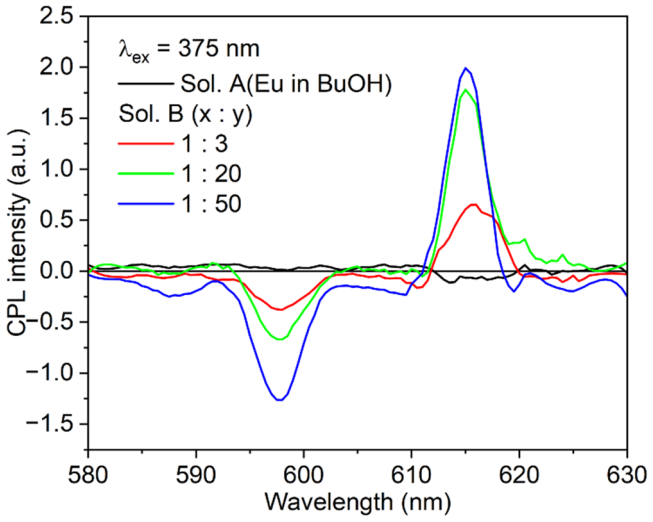

Figure 4. CPL spectra of Sol. A (Eu in BuOH) and Sol. B with varying EMImOAc concentrations (λ_{ex} = 375 nm).

3.2. Comparison of the Photophysical Properties of Sol. A (Eu in BuOH), Sol. B (1:50 in BuOH), and Sol. C (Eu in IL)

We prepared the Eu(*D*-facam)$_3$ solution by directly dissolving it into EMImOAc (Sol. C (Eu in IL)) and compared its photophysical properties with those of Sol. A (Eu in BuOH) and Sol. B (1:50). This comparison allowed us to elucidate how the solvent and IL interacted with the Eu(III) complex and influenced its overall behavior.

The absorption band of Eu(*D*-facam)$_3$ was slightly red-shifted in the IL matrix, reflecting differences in the matrix polarity and the microenvironment around the Eu(III) complexes. The shapes of the CD spectra of Sol. C (Eu in IL) were different from those of Sol. B (Figure S2). These results suggest that the structure and chirality of the complex are affected by its interactions with the surrounding solvent.

The photophysical parameters of each solution are summarized in Table 1 (calculations of these parameters and the emission decay profile of Sol. C (Eu in IL) are provided in the Supporting Information (Figure S4)). The luminescence properties of the pristine Eu(*D*-facam)$_3$ complex have been reported previously in the literature. The luminous properties observed for Sol. A (Eu in BuOH) in the present study are largely consistent with those reported for Eu(*D*-facam)$_3$ in alcohol solution [16,17]. The radiative rate (k_r) of the Eu(III) complexes increased upon interaction with the IL, indicating a decrease in the local coordination symmetry around the Eu^{3+} ion, as was observed in Figure 2. The average emission lifetimes were 66.0, 112, and 429 μs for Sol. A, Sol. B, and Sol. C, respectively, indicating an obvious extension of the lifetime in the IL medium (Sol. C). In addition, the luminescent quantum yields of the Eu(III) complexes increased upon interaction with the IL. At high EMImOAc contents, substantial changes in the photophysical parameters, including kr and knr, were observed. To examine whether these changes could be associated with aggregation or association of the Eu(*D*-facam)$_3$ complex, absorption spectra were measured while varying the concentration of Eu(*D*-facam)$_3$ at a fixed EMImOAc content (Figure S5). As a result, no significant changes in the spectral shape of the ligand-centered absorption bands were observed, and the absorbance increased linearly with concentration, following the Lambert–Beer law (Figure S5). These results suggest that, within the concentration range studied, Eu(*D*-facam)$_3$ does not form aggregated species that significantly affect its photophysical properties. Taken together, these results suggest that the nonradiative rate constant (k_{nr}) was significantly suppressed, most likely owing to the inhibition of vibrational quenching in the absence of –OH groups from 1-butanol [25,26]. Moreover, the ligand-to-Eu^{3+} ion energy-transfer efficiency (η_{sens}) was also enhanced, indicating that EMImOAc contributes not only to the luminescent process from the excited state of Eu^{3+} ions but also to the overall energy-transfer process of the Eu(III) complex. Recent investigations employing time-resolved PL spectroscopy and femtosecond transient absorption spectroscopy have demonstrated that suppression of solvent coordination enhances both the intersystem crossing (ISC) efficiency and the ligand-to-Eu^{3+} ion energy-transfer efficiency [27]. Furthermore, solvent exclusion and the formation of rigid Eu(III) complexes by interaction with organic cations have been reported [10].

Table 1. Photophysical parameters of Eu(*D*-facam)$_3$ in different solvent environments. F_{Ln}, k_r, k_{nr}, and h_{sens} calculated using Equations S1, S2, S3, and S4 in the Supplementary Information, respectively.

Solution	τ_{ave} [μs]	ϕ_{tot} [%]	ϕ_{Ln} [%]	k_r [s^{-1}]	k_{nr} [s^{-1}]	η_{sens} [%]
Sol. A (Eu in BuOH)	66.0	0.011	2.13	322	1.48×10^4	0.517
Sol. B (1:50)	112	0.881	4.64	414	8.51×10^3	19.0
Sol. C (Eu in IL)	429	6.7	20.3	473	1.86×10^3	33.0

In our system, a similar effect is likely operative. In 1-butanol, the interaction with EMImOAc partially suppresses solvent coordination, whereas in neat EMImOAc, the coordinating solvents are completely excluded. These factors collectively promote the formation of a more rigid coordination environment around the Eu^{3+} center, which may in turn enhance the ISC efficiency and the subsequent energy-transfer process. Taken together, these results indicate that the enhancement of the emission intensity observed in Figure 2 is supported not only by the reduction in the local coordination symmetry around the Eu^{3+} ion but also by photophysical factors, such as suppressed nonradiative relaxation and improved energy-transfer efficiency. It has also been reported that ILs can suppress ligand-centered nonradiative processes, thereby stabilizing the intramolecular energy-transfer pathway in other Eu(III) complex systems [28].

Figure 5 shows the CPL spectrum of Sol. C (Eu in IL). Even in the IL environment, the g_{CPL} value for the $^5D_0 \rightarrow {}^7F_1$ transition (~593 nm) reached −0.22, which, although slightly lower than the value obtained for Sol. B (−0.28), still demonstrates a pronounced chiral photoluminescent property. This result suggests that Eu(*D*-facam)$_3$ maintains a chiral local environment even in EMImOAc, indicating that the chiral structure of the complex remains stable in the IL medium.

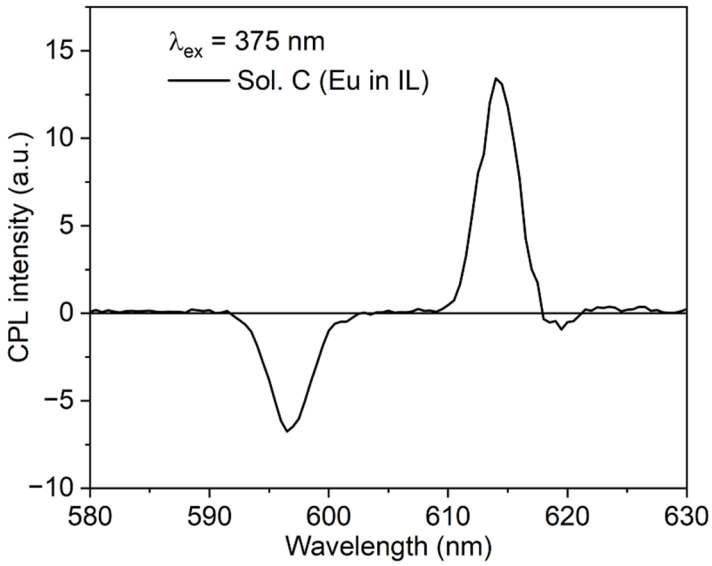

Figure 5. CPL spectrum of Sol. C (Eu in IL).

In previously reported Eu-based CPL systems, exceptionally large dissymmetry factors have been achieved by carefully designed chiral coordination environments. For example, camphor-based Eu(III) complexes bearing alkylammonium cations have been reported to exhibit very large $|g_{CPL}|$ values, reaching up to −1.54, which is among the highest values reported for Eu(III) complexes [10]. In these systems, the luminescence quantum yields are comparable to those obtained in the present study.

In contrast, although the $|g_{CPL}|$ value of Sol. C (Eu in IL) is smaller than those record values, the present system offers distinct advantages in terms of simplicity and operational robustness. Strong luminescence and CPL activity are achieved simply by mixing Eu(*D*-facam)$_3$ with EMImOAc, without the need for elaborate molecular design or rigid host matrices. Moreover, the absence of volatile molecular solvents and the low-volatility nature of the ionic liquid enables stable operation over a wide temperature range. These features place the Eu(*D*-facam)$_3$/EMImOAc system among competitive Eu-based CPL platforms, particularly for applications requiring thermal robustness and facile processability.

3.3. Temperature Dependence of Luminescent Properties

Next, the temperature dependences of the luminescence intensity and lifetime were evaluated. Because the emission intensity of Sol. A (Eu in BuOH) was quite low, a detailed discussion of its emission properties was difficult. Therefore, we focused on the luminescent properties of Sol. B (1:50) and Sol. C (Eu in IL).

Figure 6 shows the temperature-dependent changes in maximum emission intensity for the two solutions over the range from 20 to 100 °C. For Sol. B (1:50), the emission intensity decreased drastically with increasing temperature, reaching only 39% and 2.1% of its initial value at 30 and 60 °C, respectively, indicating that maintaining luminescence performance under high-temperature conditions is difficult in this system. This luminescence quenching with increasing temperature is attributed to the accelerated vibrational deactivation from the excited state of the Eu^{3+} center and the reverse energy transfer from the excited Eu^{3+} state to the T_1 state of the ligand [29]. In contrast, Sol. C (Eu in IL) retained 50% and 28% of its initial intensity at 70 and 100 °C, respectively, showing a much more gradual decrease. These results demonstrate that EMImOAc serves as an effective medium for enhancing the thermal stability of Eu(*D*-facam)$_3$, and the high emission retention of Sol. C makes it a promising candidate for luminescent devices requiring thermal robustness. In addition, although systematic thermal cycling tests were not conducted, the emission intensity of Sol. B (1:50) and Sol. C (Eu in IL) were found to be largely reversible over several heating–cooling cycles between 20 and 100 °C (Figure S6), indicating good thermal cycling stability of the luminescence.

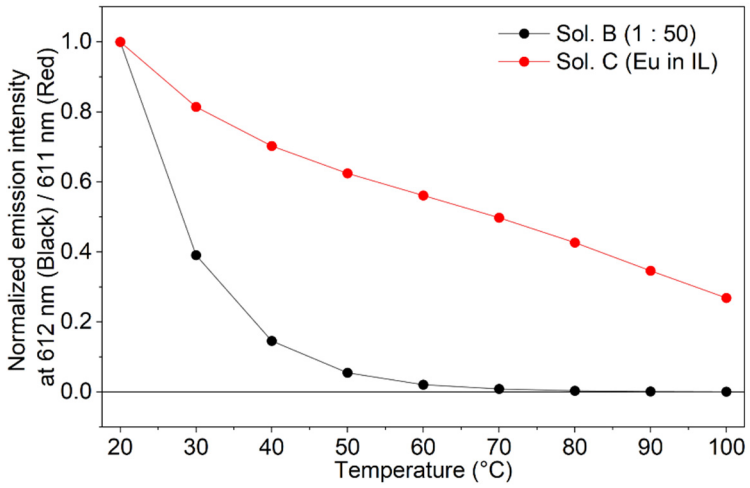

Figure 6. Comparison of temperature-dependent maximum emission intensity of Sol. B (1:50) (black) and Sol. C (Eu in IL) (red).

Figure 7 shows the temperature dependence of the emission lifetimes for the two solutions, measured from 20 to 100 °C (up to 90 °C for Sol. B (1:50)). The emission lifetimes of Sol. C (Eu in IL) decreased with increasing temperature, and this decrease generally corresponded with a decrease in emission intensity. It retained approximately 30% of its room-temperature lifetime even at 100 °C, indicating that the complex maintains a relatively long lifetime under high-temperature conditions. Sol. B (1:50) also exhibited a decrease in the emission lifetime with increasing temperature; however, the extent of this reduction was not significantly different from that observed for Sol. C. Notably, while Sol. B exhibited a remarkable decrease in emission intensity at high temperatures—for example, retaining only approximately 2% of its room-temperature intensity at 60 °C (Figure 6)—the emission lifetime remained comparatively less affected, maintaining approximately 35% of its room-temperature value at the same temperature. This suggests that the pronounced

decrease in the emission intensity of Sol. B is not primarily due to an increase in the nonradiative decay process from the $^5D_0$ excited state of the Eu^{3+} ion, but rather because of a significant reduction in the efficiency of energy transfer from the ligand excited states to the Eu^{3+} center.

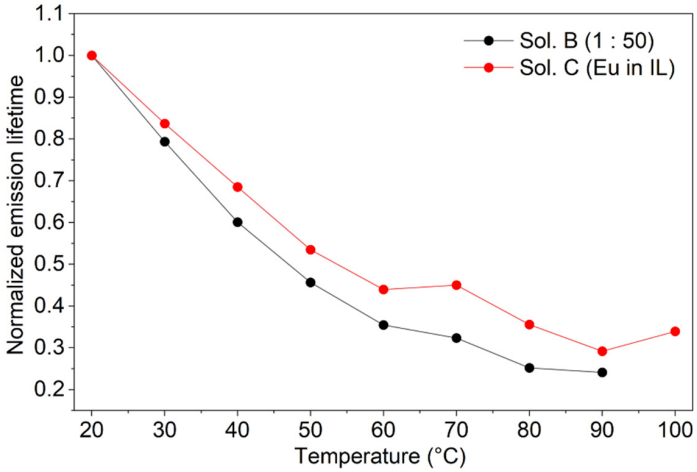

Figure 7. Comparison of temperature-dependent emission lifetimes of Sol. B (1:50) (black) and Sol. C (Eu in IL) (red).

Temperature-dependent luminescence quenching of lanthanide complexes is commonly analyzed using the Arrhenius analysis, in which thermally activated nonradiative processes are described by an activation energy. This approach has been widely applied to evaluate both emission intensity and lifetime variations with temperature in Eu(III) and other lanthanide-based luminescent systems [29,30]. Figure 8 shows the Arrhenius plots constructed from the temperature dependence of the inverse of emission intensity ($1/I_{tot}$) of Eu(*D*-facam)$_3$. Linear regression analysis of the Arrhenius plots showed good linearity within the analyzed temperature ranges (20–100 °C), with correlation coefficients (R^2) of 0.998 for Sol. B (1:50) and 0.963 for Sol. C (Eu in IL). In Sol. B, the emission intensity decreased sharply with increasing temperature, indicating that the overall nonradiative relaxation pathways of the complex were strongly promoted at high temperatures. In contrast, the slope of Sol. C was much smaller, suggesting that the increase in nonradiative processes was significantly suppressed with increasing temperature, resulting in stable emission behavior against temperature variations. These results demonstrate that EMImOAc is an effective medium for suppressing the temperature dependence of nonradiative relaxation in Eu complexes. Moreover, the stable thermal luminescence behavior of Sol. C (Eu in IL) highlighted its potential application as a temperature-responsive luminescent material.

Figure 9 shows the Arrhenius plots constructed from the inverse of the temperature-dependent emission lifetimes ($1/\tau_{ave}$). Linear regression analysis of the Arrhenius plots based on the emission lifetimes showed good linearity within the analyzed temperature range (Sol. B: 20–90 °C; Sol. C: 20–100 °C), with correlation coefficients (R^2) of 0.988 for Sol. B (1:50) and 0.956 for Sol. C (Eu in IL). It should be noted that the lifetime-based analysis reflects only the deactivation processes occurring from the $^5D_0$ excited state of Eu^{3+} ions and therefore does not include any temperature-dependent changes occurring in the ligand-centered excited states or in the ligand-to-Eu^{3+} energy-transfer processes. For both solutions, the variation in lifetime with increasing temperature was relatively small, indicating that the temperature dependence of nonradiative relaxation was weaker than that derived from the emission-intensity-based analysis (Figure 8). In particular, even in 1-butanol, complexation with EMImOAc effectively suppressed the activation of nonradiative transitions from the Eu(III) excited state and stabilized the temperature dependence.

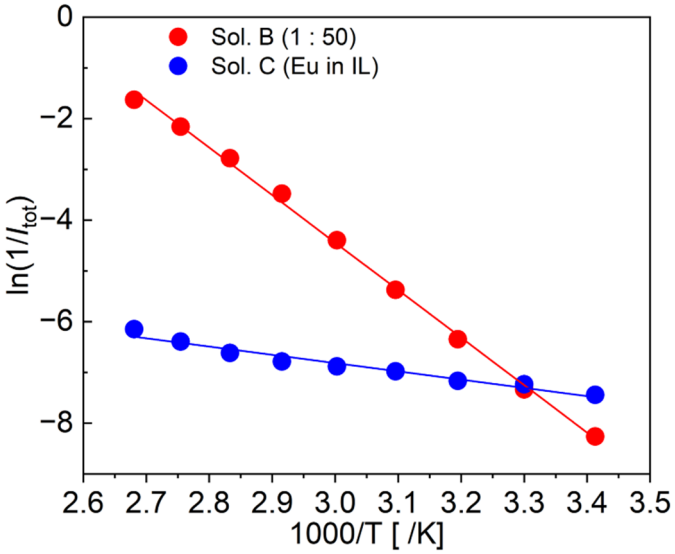

Figure 8. Arrhenius plots of emission intensity: (red) Sol. B (1:50) and (blue) Sol. C (Eu in IL).

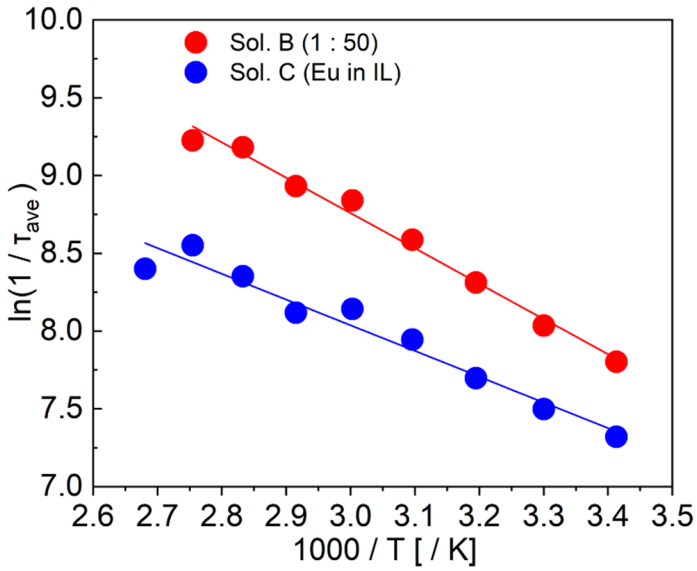

Figure 9. Arrhenius plots of emission lifetime: (red) Sol. B (1:50) and (blue) Sol. C (Eu in IL).

The activation energies of the nonradiative processes were determined from the temperature dependence of the emission intensity and lifetime based on the Arrhenius equations ((2) for emission intensity and (3) for emission lifetime), and the differences in photophysical properties between the two solutions were examined.

$$ln\frac{1}{I_{tot}} = lnA - \frac{E_a}{R}\frac{1}{T} \quad (2)$$

$$ln\frac{1}{\tau_{ave}} = lnA' - \frac{E'_a}{R}\frac{1}{T} \quad (3)$$

Assuming that the absorption of the ligand is temperature-independent, the inverse of total emission intensity ($1/I_{tot}$) can be approximated by the emission quantum yield (F_{tot}) and expressed as the product of the radiative rate constant (k_r), emission lifetime (τ_{ave}), and the energy-transfer efficiency from the ligand to the Eu^{3+} ion (η_{sens}), as shown in Equation (4).

$$\frac{1}{I_{tot}} \approx \frac{1}{\Phi_{tot}} = \frac{1}{\tau \cdot k_r \cdot \eta_{sens}} = \frac{k_r + k_{nr}}{k_r \cdot \eta_{sens}} \quad (4)$$

The inverse of the emission lifetime ($1/\tau_{ave}$) is represented by the following kinetic relationship.

$$\frac{1}{\tau_{ave}} = k_r + k_{nr} \quad (5)$$

Because the radiative rate constant (k_r) is known to be less temperature-dependent [30], the activation energy obtained from the Arrhenius analysis of the emission lifetime using Equation (3) mainly reflects the temperature dependence of the nonradiative decay rate constant (k_{nr}) corresponding to the local relaxation pathways from the $^5D_0$ level of Eu(III) to the ground state. In contrast, the analysis based on emission intensity (Equation (2)) reflects not only the temperature dependence of k_{nr} but also the overall energy-transfer processes within the complex, including radiative and nonradiative transitions from the ligand excited states (S_1 and T_1) and the subsequent energy transfer from the ligand to the Eu^{3+} ion. These combined contributions reflect the temperature dependence of the overall energy-transfer dynamics within the system. The difference between the activation energies obtained using Equations (2) and (3) are therefore considered to primarily reflect the temperature dependence of the rate constants associated with the processes that contribute to the energy-transfer efficiency (η_{sens}). Accordingly, a comparison of these two Arrhenius analyses allows the evaluation of how the energy-transfer efficiency between the ligand and Eu^{3+} ion varies with temperature. Table 2 lists the activation energies of Sol. B (1:50) and Sol. C (Eu in IL) calculated from the emission intensity (E_a) and emission lifetime (E'_a) dependence.

Table 2. Comparison of activation energies for Sol. B (1:50) and Sol. C (Eu in IL).

Solution	E_a (Emission Intensity)	E'_a (Emission Lifetime)
Sol. B (1:50)	77.8 kJmol^{-1}	18.9 kJmol^{-1}
Sol. C (Eu in IL)	13.5 kJmol^{-1}	13.7 kJmol^{-1}

In Sol. B (1:50), the activation energy determined from the emission lifetime was relatively low (18.9 kJ mol^{-1}), whereas that derived from the emission intensity was remarkably high (77.8 kJ mol^{-1}). This large discrepancy suggests a significant decrease in the energy-transfer efficiency (η_{sens}) from the ligand to the Eu^{3+} ion with increasing temperature. In contrast, in Sol. C (Eu in IL), the activation energies derived from both emission lifetime (13.7 kJ mol^{-1}) and emission intensity (13.5 kJ mol^{-1}) were nearly identical, indicating that the ligand-related nonradiative processes exhibit minimal temperature dependence. The marked difference in temperature dependence of η_{sens} between Sol. B and Sol. C can likely be attributed to the distinct coordination environments created by the two solvent systems. In particular, the IL medium provided a rigid complexation environment that stabilized the ligand excited states and suppressed nonradiative deactivation pathways at higher temperatures. This behavior contrasts with that in 1-butanol, in which solvent coordination cannot be completely eliminated. These results clearly demonstrate that ILs offer a thermally robust environment that maintains highly efficient ligand-to-Eu^{3+} ion energy transfer.

From a temperature-sensing perspective, photophysical parameters other than emission intensity are more suitable for reliable readout. In particular, the long emission lifetime characteristic of trivalent lanthanide ions enables time-gated detection, allowing efficient discrimination of the Eu^{3+} emission from background fluorescence. In addition, circularly polarized luminescence provides an orthogonal optical parameter that facilitates discrimination from other emissive components, such as unpolarized or linearly polarized light, while both the emission lifetime and the dissymmetry factor (g_{CPL}) are intrinsically

independent of excitation intensity, making them promising metrics for stable and robust temperature sensing.

3.4. Photostability Under Continuous UV Irradiation

To evaluate the photostability of the Eu(III) complexes, the emission spectra were continuously monitored under UV irradiation (centered at 365 nm) for up to 5 h, and the results are shown in Figure 10. While a pronounced decrease in emission intensity was observed for Sol. A (Eu in BuOH), the EMImOAc-containing systems exhibited significantly improved photostability. In particular, Sol. C (Eu in IL) retained most of its initial emission intensity even after prolonged UV exposure. These results indicate that the ionic liquid environment effectively suppresses photodegradation and provides enhanced resistance against prolonged excitation.

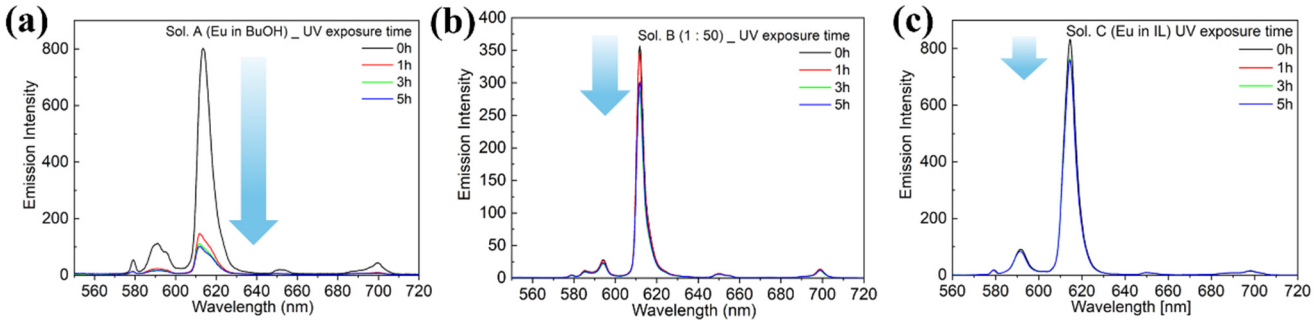

Figure 10. Emission spectra of (**a**) Sol. A (Eu in BuOH), (**b**) Sol. B (1:50), and (**c**) Sol. C (Eu in IL) recorded under continuous UV irradiation for up to 5 h.

4. Conclusions

We demonstrated that the hybridization of Eu(*D*-facam)$_3$ with EMImOAc significantly enhances luminescence intensity, circularly polarized emission, and thermal robustness. In 1-butanol, EMImOAc addition reduced the local coordination symmetry around the Eu^{3+} ion and suppressed the –OH vibration-induced nonradiative decay, leading to an increased lifetime and improved emission. In pure EMImOAc, the activation energies derived from both emission lifetime and intensity were similarly low, indicating that nonradiative decay from the ligand's excited states exhibits negligible temperature dependence, while the ligand-to-Eu^{3+} ion energy-transfer efficiency (η_{sens}) remains stable over a wide temperature range. The combined effect results in a chiral Eu(III) complex system with high thermal stability and efficient emission that is suitable for advanced luminescent and chiroptical applications.

Supplementary Materials: The following supporting information can be downloaded at: https://www.mdpi.com/article/10.3390/physchem6010013/s1, Figure S1. Absorption and CD spectra of Sol. B with various mixing ratios. Figure S2. Absorption and CD spectra of Sol. A (Eu in BuOH), Sol. B (1:50) and Sol. C (Eu in IL). Figure S3. Experimental ESI-MS spectra of (a) Sol. A (Eu in BuOH) and (b)Sol. B (1:50). Figure S4. Emission decay profile of Sol. C (Eu in IL) (λ_{em} = 612 nm). Figure S5. The corresponding absorbance at 310 nm plotted as a function of Eu(D-facam)3 concentration. (Inset) Absorption spectra of Eu(D-facam)3 at different concentrations with a fixed EMImOAc concentration (10 mM). Figure S6. Emission intensity monitored during repeated heating–cooling cycles between 20 and 100 °C for (a) Sol. B (1:50) and (b) Sol. C (Eu in IL).

Author Contributions: A.S.: Preparation of samples, measurements of photophysical properties, and draft writing. Z.L.: Technical guidance, scientific discussion, and measurements of photophysical properties. N.K.: Scientific discussion and research planning. K.N.: Project management, application

of research fund, and paper refinement. All authors have read and agreed to the published version of the manuscript.

Funding: This study was partly supported by JSPS KAKENHI (Grant No. 23K04871 and 23K23422), New Energy and Industrial Technology Development Organization (NEDO) (JPNP20004), Iketani Science and Technology Foundation, and Izumi Science and Technology Foundation.

Data Availability Statement: The original contributions presented in this study are included in the article/Supplementary Material. Further inquiries can be directed to the corresponding author(s).

Conflicts of Interest: There are no conflicts of interest to declare.

References

1. Kozlov, M.I.; Vashchenko, A.A.; Pavlov, A.A.; Goloveshkin, A.S.; Latipov, E.V.; Kuzmina, N.P.; Utochnikova, V.V. The increase of europium-based OLED luminance through reducing the excited state lifetime by mixed-ligand complex formation. *Phys. Chem. Chem. Phys.* **2023**, *25*, 20042–20048. [CrossRef]
2. Zhao, B.; Zhang, H.; Miao, Y.; Wang, Z.; Gao, L.; Wang, H.; Hao, Y.; Xu, B.; Li, W. Low turn-on voltage and low roll-off rare earth europium complex-based organic light-emitting diodes with exciplex as the host. *J. Mater. Chem. C* **2017**, *5*, 12182–12188. [CrossRef]
3. Tsukube, H.; Shinoda, S. Lanthanide Complexes in Molecular Recognition and Chirality Sensing of Biological Substrates. *Chem. Rev.* **2002**, *102*, 2389–2404. [CrossRef] [PubMed]
4. Yuan, J.; Wang, G. Lanthanide Complex-Based Fluorescence Label for Time-Resolved Fluorescence Bioassay. *J. Fluoresc.* **2005**, *15*, 559–568. [CrossRef]
5. Hasegawa, Y.; Kitagawa, Y. Luminescent lanthanide coordination polymers with transformative energy transfer processes for physical and chemical sensing applications. *J. Photochem. Photobiol. C* **2022**, *51*, 100485. [CrossRef]
6. Muller, G. Luminescent chiral lanthanide (III) complexes as potential molecular probes. *Dalton Trans.* **2009**, 9692–9707. [CrossRef] [PubMed]
7. Kumar, J.; Nakashima, T.; Kawai, T. Circularly Polarized Luminescence in Chiral Molecules and Supramolecular Assemblies. *J. Phys. Chem. Lett.* **2015**, *6*, 3445–3452. [CrossRef]
8. Duan, X.-F.; Ji, H.; Zhou, L.-P.; Hu, S.-J.; Fu, J.; Duan, P.; Guo, X.-Q.; Sun, Q.-F. Upconverted Circularly Polarized Luminescence on Chiral Lanthanide-Organic Tetrahedral Complexes. *CCS Chem.* **2025**, *7*, 1972–1980. [CrossRef]
9. Lunkley, J.L.; Shirotani, D.; Yamanari, K.; Kaizaki, S.; Muller, G. Extraordinary Circularly Polarized Luminescence Activity Exhibited by Cesium Tetrakis(3-heptafluoro-butylryl-(+)-camphorato) Eu(III) Complexes in EtOH and $CHCl_3$ Solutions. *J. Am. Chem. Soc.* **2008**, *130*, 13814–13815. [CrossRef]
10. Tsurui, M.; Takizawa, R.; Kitagawa, Y.; Wang, M.; Kobayashi, M.; Taketsugu, T.; Hasegawa, Y. Inside Back Cover: Chiral Tetrakis Eu(III) Complexes with Ammonium Cations for Improved Circularly Polarized Luminescence. *Angew. Chem. Int. Ed.* **2024**, *63*, e202405584. [CrossRef]
11. Zhang, D.-W.; Li, M.; Chen, C.-F. Recent advances in circularly polarized electroluminescence based on organic light-emitting diodes. *Chem. Soc. Rev.* **2020**, *49*, 1331–1343. [CrossRef]
12. Li, Z.; Nakamura, K.; Kobayashi, N. Thermally stable and strongly emitted CPL in Eu(*D*-facam)$_3$ hybrid solids with an alkylammonium salt. *J. Mater. Chem. C* **2023**, *11*, 118–126. [CrossRef]
13. YHirai; Nakanishi, T.; Kitagawa, Y.; Fushimi, K.; Seki, T.; Ito, H.; Hasegawa, Y. Luminescent Europium(III) Coordination Zippers Linked with Thiophene-Based Bridges. *Angew. Chem. Int. Ed.* **2016**, *55*, 12059–12062.
14. Minami, H.; Itamoto, N.; Watanabe, W.; Li, Z.; Nakamura, K.; Kobayashi, N. Chiroptical property enhancement of chiral Eu(III) complex upon association with DNA-CTMA. *Sci. Rep.* **2020**, *10*, 18917. [CrossRef] [PubMed]
15. Matsumiya, M.; Kazama, R.; Tsunashima, K. Analysis of Thermodynamic Properties for Rare Earth Complexes in Ionic Liquids by Raman Spectroscopy and DFT Calculation. *J. Appl. Solut. Chem. Model.* **2016**, *5*, 157–167. [CrossRef]
16. Minami, M.; Miyazato, M.; Li, Z.; Nakamura, K.; Kobayashi, N. Alkyl ammonium ion-induced drastic emission enhancement of Eu (*D*-facam) $_3$ in 1-butanol. *Chem. Commun.* **2020**, *56*, 13532–13535. [CrossRef]
17. Li, Z.; Minami, H.; Nakamura, K.; Kobayashi, N. Anion-Dependent Outstanding Luminescence Enhancement of Eu(*D*-facam)$_3$ Upon Coexistence With the Tetramethylammonium Cation. *ChemPhysChem* **2021**, *22*, 2511–2516. [CrossRef] [PubMed]
18. Xu, C.; Cheng, Z. Thermal Stability of Ionic Liquids: Current Status and Prospects for Future Development. *Processes* **2021**, *9*, 337. [CrossRef]
19. Fabrizi, I.; Di Muzio, S.; Ramondo, F.; Trequattrini, F.; Palumbo, O.; Paolone, A. Vapor Pressure of Ionic Liquids with a Common Tetrabutylammonium Cation and Three Different Anions. *Appl. Sci.* **2025**, *15*, 6040. [CrossRef]

20. Kim, Y.; Ohmagari, H.; Saso, A.; Tamaoki, N.; Hasegawa, M. Electrofluorochromic Device Based on a Redox-Active Europium(III) Complex. *ACS Appl. Mater. Interfaces* **2020**, *12*, 46390–46396. [CrossRef]
21. Tsumatori, H.; Nakashima, T.; Kawai, T. Observation of Chiral Aggregate Growth of Perylene Derivative in Opaque Solution by Circularly Polarized Luminescence. *Org. Lett.* **2010**, *12*, 2362–2365. [CrossRef]
22. Puntus, L.N.; Pekareva, I.S.; Lyssenko, K.A.; Shaplov, A.S.; Lozinskaya, E.I.; Zdvizhkov, A.T.; Buzin, M.I.; Vygodskii, Y.S. Influence of ionic liquid anion nature on the properties of Eu-containing luminescent materials. *Opt. Mater.* **2010**, *32*, 707–710. [CrossRef]
23. Sravani, V.V.; Gupta, S.K.; Sreenivasulu, B.; Rao, C.V.S.B.; Suresh, A.; Sivaramann, N. Luminescence properties of europium (III)-based metal–organic frameworks: Influence of varied organic linkers. *J. Mol. Struct.* **2022**, *1269*, 133767. [CrossRef]
24. Yu, Y.; Weng, F.; Chen, D.; Huang, P.; Wang, Y. Optical spectroscopy investigation on distribution of Eu3+ in nanostructured glass ceramics. *J. Appl. Phys.* **2010**, *107*, 093504. [CrossRef]
25. Beeby, A.; Clarkson, I.M.; Dickins, R.S.; Faulkner, S.; Parker, D.; Royle, L.; de Sousa, A.S.; Williams, J.A.G.; Woods, M. Non-radiative deactivation of the excited states of europium, terbium and ytterbium complexes by proximate energy-matched OH, NH and CH oscillators: An improved luminescence method for establishing solution hydration states. *J. Chem. Soc. Perkin Trans. 2* **1999**, 493–504. [CrossRef]
26. Haas, Y.; Stein, G. Radiative and nonradiative pathways in solutions. Excited states of the europium (III) ion. *J. Phys. Chem.* **1972**, *76*, 1093–1104. [CrossRef]
27. Miyazaki, S.; Gotanda, M.; Kitagawa, Y.; Hasegawa, Y.; Miyata, K.; Onda, K. Full picture of energy transfer in a trivalent Europium complex with bidentate β-diketonate ligand. *J. Phys. Chem. Lett.* **2024**, *15*, 10718–10724. [CrossRef]
28. Hasegawa, Y.; Ishii, A.; Inazuka, Y.; Yajima, N.; Kawaguchi, S.; Sugimoto, K.; Hasegawa, M. The enhanced intramolecular energy transfer and strengthened ff luminescence of a stable helical Eu complex in ionic liquids. *Molecules* **2018**, *23*, 55. [CrossRef] [PubMed]
29. Hasegawa, Y.; Kitagawa, Y. Luminescent lanthanide complexes, clusters, coordination polymers and metal-organic frameworks with temperature-sensing properties. *J. Mater. Chem. C* **2019**, *7*, 7494–7511. [CrossRef]
30. Thor, W.; Kai, H.-Y.; Zhang, Y.; Wong, K.-L.; Tanner, P.A. Thermally Activated Photophysical Processes of Organolanthanide Complexes in Solution. *J. Phys. Chem. Lett.* **2022**, *13*, 4800–4806. [CrossRef]

Disclaimer/Publisher's Note: The statements, opinions and data contained in all publications are solely those of the individual author(s) and contributor(s) and not of MDPI and/or the editor(s). MDPI and/or the editor(s) disclaim responsibility for any injury to people or property resulting from any ideas, methods, instructions or products referred to in the content.